Article ID: 1007-8827(2012)04-0271-07

Dispersion of expanded graphite as nanoplatelets in a copolymer matrix and its effect on thermal stability, electrical conductivity and permeability

Gyanaranjan Prusty[1], Sarat K Swain[1,2]

(1. *Department of Chemistry, North Orissa University, Takatpur, Baripada* 757003, *India*;
2. *Department of Chemistry, Veer Surendra Sai University of Technology, Burla, Sambalpur* 768018, *India*)

Abstract: Expanded graphite/polyacrylonitrile-co-poly (methyl methacrylate) (EG/PAN-co-PMMA) composites were prepared by the incorporation of EG at various concentrations (1, 2, 3, and 4%, w/w) into PAN-co-PMMA by an in situ emulsifier-free emulsion polymerization method. As-synthesized composites were characterized by UV/VIS and FT-IR, XRD, SEM, TEM and TGA. The thermal stability of the copolymer was significantly improved by the addition of EG. The oxygen permeabilities of the composites were substantially reduced and the electrical conductivities of the composites were significantly increased by increasing the EG content.

Keywords: Nanocomposite; PAN-co-PMMA; Expanded graphite; Oxygen permeability; Thermogravimetric analysis
CLC number: TB 332 **Document code**: A

1 Introduction

Nanocomposites are a new class of materials that contain at least one filler in the nanometer range[1]. The nanocomposites containing layered silicates exhibit a markedly superior mechanical, thermal, and barrier performance in comparison with conventional composites[2-3], but they do not possess electrical conductivity. Different conductive fillers such as carbon black and carbon nanotubes have been extensively explored for their composite components[4-5]. These fillers effectively improve the conductivity of the composites. The significant improvement in electrical conductivity arising from the increase in the filler content was observed for most composites, and it was explained by the percolation transition of the conductive network formation[6].

Natural graphite possesses effective electrical conductivity (10^4 S/cm at ambient temperature) as well as a good layered structure. These layers are bonded by weak van der Waals forces. Consequently, different oxidizing agents such as sulfuric acid and nitric acid can be easily intercalated into graphite interlayers, forming graphite intercalation compounds (GICs). Expanded graphite (EG) possessing a high aspect ratio and an excellent electrical conductivity can be produced by exfoliating GICs through rapid heating in a furnace. Graphene sheets are two-dimensional layers of sp^2-bonded carbon atoms that possess a wide range of unusual properties[7-9]. One possible method of utilizing these properties for applications would be by incorporating graphene sheets in a composite material.

At present, graphene continues to attract considerable attention because of its outstanding electrical properties as well as high aspect ratio, which makes it an ideal filler for developing functional and structural graphene-reinforced composites. The incorporation of graphene into polymer matrices[10-13] remarkably improves the properties of the materials. Copolymerization is the most general and powerful method that is used to systematically change the properties of polymers, and it is also widely used in the production of commercial polymers. Polymers containing conducting fillers and conducting polymer composites have been extensively studied because of their potential applications in light-emitting devices, batteries, electromagnetic shielding, anti-static and corrosion-resistant coatings, and other functional applications[14-16].

Polymer-based nanocomposites containing

Received date: 2012-01-27; **Revised date**: 2012-03-15

Corresponding author: Sarat K Swain. Fax: 06792-255127, E-mail: swainsk2@yahoo.co.in

Author introduction: Gyanaranjan Prusty (1985-), male, Doctoral Candidate, engaged in the research in the field on polymer nanocomposites. E-mail: gyanaranjan.bapu@gmail.com

English edition available online ScienceDirect (http://www.sciencedirect.com/science/journal/18725805).
DOI: 10.1016/S1872-5805(12)60017-1

strong, durable, and multifunctional nanoparticles such as silicates[17-18], fullerenes[19], carbon nanotubes[20-22], and graphene sheets[23-24] have been considered as promising advanced materials, because a significant improvement in the properties of the nanocomposites can be achieved, compared with conventional composites, when nanoparticles are homogeneously dispersed in a polymer matrix.

In the present study, EG-reinforced polyacrylonitrile-co-poly (methyl methacrylate) (PAN-co-PMMA) composites were prepared by incorporating EG sheets into a copolymer matrix. The synthesized composites exhibited an appreciable enhancement of both thermal and conductive properties. The substantial reduction in the oxygen-barrier properties was significant and new and aimed at studying the permeable properties of PAN-co-PMMA/EG nanocomposites.

2 Experimental

2.1 Materials

Acrylonitrile (AN, Merck, Germany) and methylmethacrylate (MMA, Himedia, India) were purchased and washed with 3 mass% phosphoric acid and 5 mass% sodium hydroxide followed by treatment with double-distilled water for further purification. Concentrated sulfuric acid (H_2SO_4), concentrated nitric acid (HNO_3), potassium persulphate ($K_2S_2O_8$), and ammonium ferrous sulphate were considered the analytical reagent grade chemicals that were directly used without any further purification. Graphite fine powder with an average diameter of 500 μm that was used for preparing EG was purchased from Loba Chemical Pvt. Ltd. (India).

2.2 Preparation of expanded graphite

Raw graphite was first dried in a vacuum oven for 24 h at 100 ℃. Then, a mixture consisting of concentrated H_2SO_4 and concentrated HNO_3 (4∶1 v/v) was slowly added to a glass flask containing graphite powder to form an oxidized graphite suspension, which was filtered, washed with deionized water, and dried at 100 ℃ for 24 h. The resulting GIC was subjected to a thermal shock at 900 ℃ for one min in a muffle furnace in a nitrogen atmosphere with the aim of producing EG.

2.3 Preparation of PAN-co-PMMA/EG nanocomposites

PAN-co-PMMA/EG nanocomposites were synthesized by an in situ polymerization technique. As-prepared EG was dispersed in deionized water via stirring for 30 min with ultrasound (120 W/80 kHz) treatment for 15 min. Then, the monomers AN and MMA were added to the suspension under stirring, followed by treatment with ultrasound for 15 min. Next, the calculated amount of $K_2S_2O_8$ was slowly added to the reaction vessel. The polymerization reaction was carried out at 333 K with stirring for 3 h. The process was terminated by the addition of 0.1M of ammonium ferrous sulphate solution. The product was filtered, washed with deionized water, and dried in an oven for 48 h. The detailed synthetic process for the nanocomposites is illustrated in Scheme 1 and Table 1.

Table 1 The variation in the concentrations of MMA, AN and $K_2S_2O_8$ at different mass fractions of EG and the conversion of monomers during the synthesis of PAN-co-PMMA/EG nanocomposites at 65 ℃

Samples	C_{MMA}/mol·dm^{-3}	C_{AN}/mol·dm^{-3}	$C_{K_2S_2O_8}$/mol·dm^{-3}	EG content w/%	Conversion η/%
PAN-co-PMMA-1	1.41	1.51	1×10^{-2}	0	53.2
PAN-co-PMMA-2	0.94	2.25	1×10^{-2}	0	50.5
PAN-co-PMMA-3	1.41	1.51	1.5×10^{-2}	0	65.8
PAN-co-PMMA-4	0.94	2.25	1.5×10^{-2}	0	55.4
PAN-co-PMMA/EG-1	1.41	1.51	1.5×10^{-2}	1	60.4
PAN-co-PMMA/EG-2	1.41	1.51	1.5×10^{-2}	2	62.8
PAN-co-PMMA/EG-3	1.41	1.51	1.5×10^{-2}	3	63.3
PAN-co-PMMA /EG-4	1.41	1.51	1.5×10^{-2}	4	65.5

2.4 Characterization

The UV-visible absorption spectra of EG, PAN-co-PMMA, and PAN-co-PMMA/EG were measured with the help of a shimadzu (Model no. 2450, Japan) UV-visible spectrophotometer. In order to confirm the chemical interaction between EG and the polymer matrix, FTIR spectroscopy was performed. The FTIR spectra of the composites were recorded in a "Perkin-Elmer" (Model no. paragon-500) spectrometer in KBr medium at room temperature in the wavenumber region of 4 000-400 cm^{-1}. The synthesized PAN-co-PMMA/EG composites were ground into powder with a pestle under uniform pressure. The powdered materials were placed in a sample holder for X-ray diffractometry. Powder XRD data were collected in a reflection mode in an angular $2\theta = 40°$ at ambient temperature by a Rigaku X-ray (Model no. P-DD966) diffractometer, which was operated at a

Cu$K\alpha$ wave length of 0.154 nm. The radiation from the anode was obtained at 40 kV and 15 mA. The diffractometer was equipped with a 1° divergence slit, a 16 mm beam bask, a 0.2 mm receiving slit, and a scatter slit of 1°. The morphology and dispersion of the EG in PAN-co-PMMA were investigated by using a scanning electron microscopy (SEM) that utilized a "JEOL-JSM"-5800 model. The conductance and impedance were measured with the LCR-Hi-TESTER (Japan, HOIKI, Model 3532-50) that possessed two probes. The measurements of the oxygen permeability of the nanocomposite films were performed with ASTM F 316-86 by using an oxygen permeation analyzer (PMI instrument, model GP-201-A, NY, USA). The sample films of a thickness of 0.5 mm were prepared at 218 ℃ and 10 MPa. The average permeability of five similar samples was reported as a comparison.

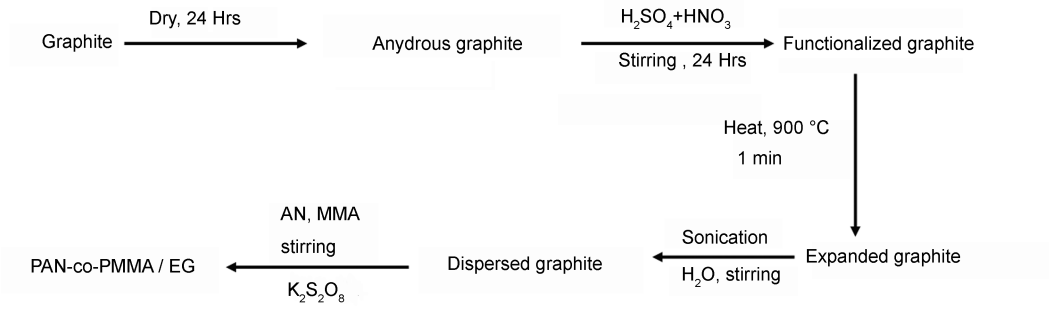

Scheme 1　Synthetic process for PAN-co-PMMA/EG nanocomposites

3　Results and discussion

3.1　Characterization by UV-visible and FTIR spectra

Fig. 1 depicts the UV-vis spectra of the samples, providing the evidence of chemical interactions between PAN-co-PMMA and EG. The curve of PAN-co-PMMA exhibits an absorption at 210 nm, whereas PAN-co-PMMA/EG exhibits an absorption at 238 nm. The red shift observed in the nanocomposites may be caused by the electronic conjugation within the carbon framework, that is, of the graphene sheets with the cyanide group of polyacrylonitrile. This result is in agreement with that published in earlier reports[25-26].

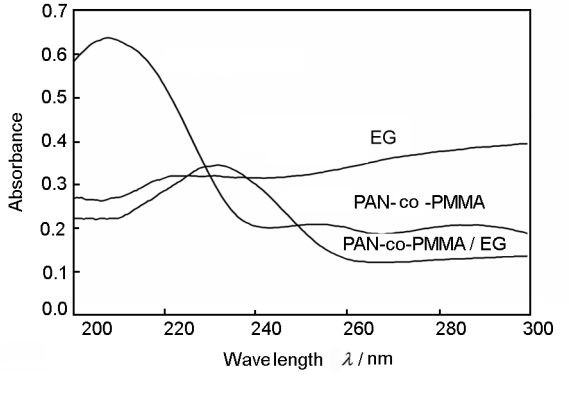

Fig. 1　UV-vis spectra of EG, PAN-co-PMMA and PAN-co-PMMA/EG nanocomposites

The FTIR spectra of EG, PAN, PMMA, PAN-co-PMMA, and PAN-co-PMMA/EG were studied with the aim of identifying the functionalized groups present in different samples (Fig. 2). From the FTIR spectra, it was observed that PAN displays a characteristic absorption peak at 2 260 cm^{-1} which is ascribed to —C≡N stretching, whereas PMMA shows an absorption peak at 1 750 cm^{-1} that is associated with C═O stretching. The FTIR spectrum of synthesized PAN-co-PMMA exhibited two absorption bands at 2 260 cm^{-1} for the —C≡N group of PAN and at 1 750 cm^{-1}, for the C═O group of PMMA. The presence of these two absorption peaks in PAN-co-PMMA indicated the formation of copolymers. In the PAN-co-PMMA/EG composite, the absorption peaks were similar to PAN-co-PMMA, except that the absorption bands assigned to the nitrile and carbonyl groups at 2 260 and 1 750 cm^{-1} for PAN-co-PMMA shifted to lower wave numbers 2 240 and 1 735 cm^{-1}, respectively. This blue shift may be caused by the interaction between the nitrile and carbonyl groups of PAN-co-PMMA with EG, which is in agreement with the UV results.

3.2　Structure of nanocomposites

The XRD petterns of raw graphite, EG, PAN-co-PMMA, and PAN-co-PMMA/EG nanocomposites are depicted in Fig. 3. The raw graphite exhibits a sharp diffraction peak at 2θ = 26.36°. The corresponding d-spacing was calculated to be 0.337 7 nm, which was the interplanar distance between the graphene sheets in the graphite. From the XRD pettern

of EG, the broad peak at $2\theta = 15.7°$, in addition to the peak at $2\theta = 26.36°$ of raw graphite, may be attributed to the change in the interlayer spacing of EG, which had been expanded to different degrees. A strong peak at a 2θ value of 9.95° in the XRD pattern of the PAN-co-PMMA and PAN-co-PMMA/EG composites was due to the crystallinity of PAN-co-PMMA. However, the peak at 21.48° in the PAN-co-PMMA/EG nanocomposite was apparent. The shifting of the graphite peak to a lower 2θ value (from 26.36° to 21.48°) was explained by the expansion of the interplanar d-spacing observed in the graphene sheets. It was also found that the intensity of the graphite peak in the nanocomposites is less than that of the raw graphite. This may be ascribed to the change in crystallinity as a result of the dispersion of EG with the copolymer in the form of nanocomposites. The result revealed that the PAN-co-PMMA matrix was intercalated within the graphite nanoplatelets.

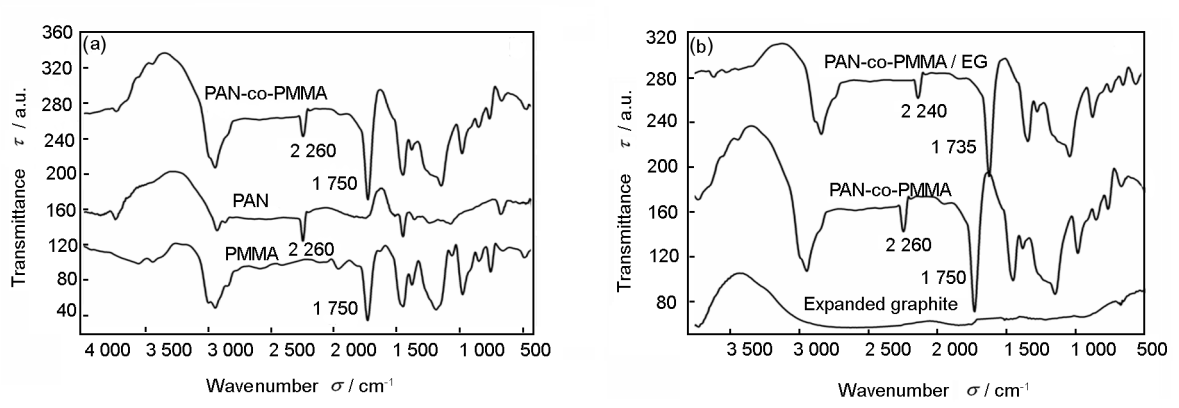

Fig. 2 FTIR spectra of (a) PMMA, PAN and PAN-co-PMMA (b) EG, PAN-co-PMMA and PAN-co-PMMA/EG nanocomposites

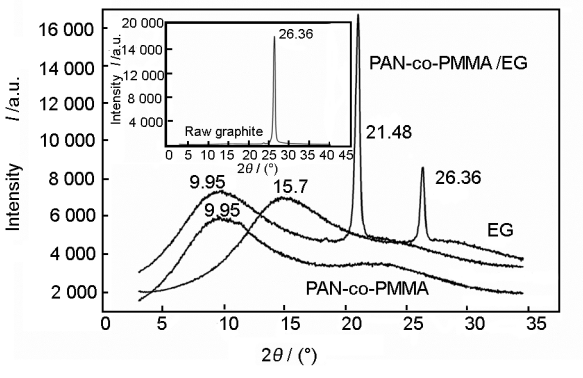

Fig. 3 X-ray diffraction of raw graphite, EG, PAN-co-PMMA and PAN-co-PMMA/EG nanocomposites

The SEM images of EG and PAN-co-PMMA/EG nanocomposite are depicted in Fig. 4a and b. It was revealed that the EG was completely distorted into sheets with a thickness of 30-80 nm, which were named graphite nanosheets. Single sheets with a thickness of about 70 nm were found, indicating that the EG is composed of graphene nanosheets. HRSEM image (Fig. 4b) taken of the composite revealed that the graphene nanosheets were well dispersed in the copolymer matrix. The TEM image of PAN-co-PMMA/EG (Fig. 5) gives a visual representation of the dispersion of graphite platelets within the copolymer matrix.

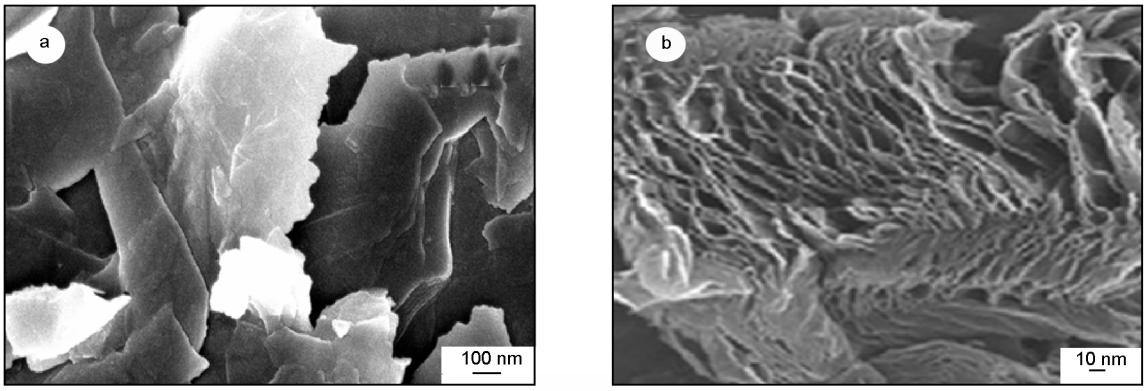

Fig. 4 SEM images of (a) EG and (b) PAN-co-PMMA/EG nanocomposites with 4 mass% graphite nanosheets

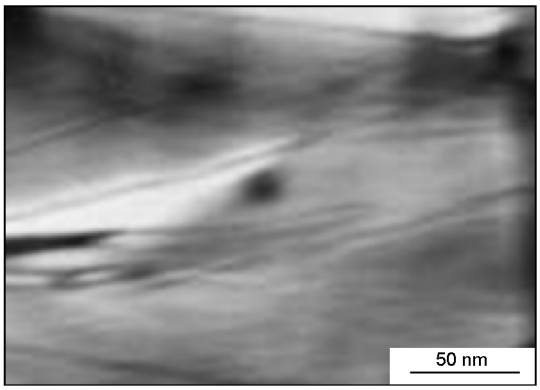

Fig. 5　TEM image of PAN-co-PMMA/EG composite with 4 mass% graphite nanosheets

The platelets are clearly seen as dark stripes, exhibiting the extent of exfoliation; the graphite platelets are exfoliated within the polymer matrix; and some black spots that are observed may be due to the local aggregation of the graphite in the nanocomposites.

3.3　Thermal properties of PAN-co-PMMA/EG nanocomposites

Thermogravimetric analysis (TGA) was further used to characterize the thermal properties of EG, PAN-co-PMMA, and PAN-co-PMMA/EG (Fig. 6). It was observed that the decomposition of the PAN-co-PMMA/EG composite was shifted toward a higher temperature as compared with PAN-co-PMMA. The thermal decomposition of PAN-co-PMMA occurred in two steps with a maximum decomposition occurring at 320 ℃. The first step is caused by water loss, and the second is ascribed to a decomposition of PAN-co-PMMA. One-step degradation was observed in the case of EG due to water loss. The thermal degradation of PAN-co-PMMA/EG occurred in two steps with a maximum degradation occurring at 350 ℃.

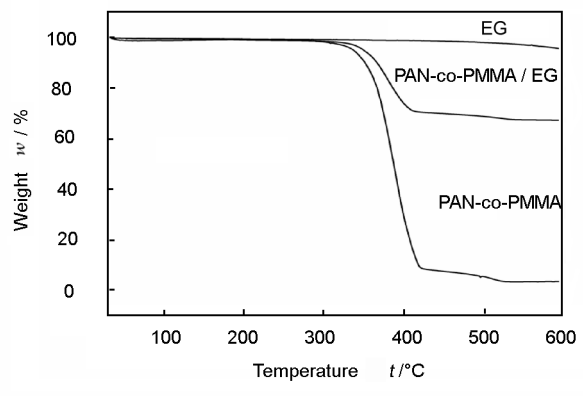

Fig. 6　TGA curves of EG, PAN-co-PMMA and PAN-co-PMMA/EG nanocomposites

The first step is caused by water loss, and the second is ascribed to the decomposition of PAN-co-PMMA/EG. The PAN-co-PMMA decomposed completely, and the residue was 0; whereas the PAN-co-PMMA/EG composite decomposed partially with a residue of 70%. The residue percentage was calculated by taking the initial sample weight for TGA. A larger residue for the PAN-co-PMMA/EG composite could be accounted for by a higher thermal stability resulting from a good dispersion of graphite with the copolymer matrix and a strong chemical interaction between the copolymer and EG, as evidenced by the FTIR with a shifting of the carbonyl and nitrile peak to lower wave numbers.

3.4　Electrical properties of PAN-co-PMMA/EG nanocomposites

The addition of conductive particles to an insulating polymer can result in an electrically conductive composite if the particle concentration exceeds the percolation threshold, which is defined as the particle volume fraction required for the formation of a three-dimensional conductive network of the fillers within the polymer matrix. The percolation threshold is characterized by a sharp jump in the conductivity by many orders of magnitude, which is attributed to the formation of a conductive network within the matrix. The percolation threshold for electrical conductivity in polymer/graphite composites is influenced by several characteristics of EG, such as aspect ratio and dispersity. The EG/polymer composites exhibit a very low percolation threshold for electrical conductivity because of the large aspect ratio and the nanoscale dimension of EG.

The electrical conductivity of PAN-co-PMMA/EG nanocomposites was enhanced, due to a better dispersion of EG in the polymer matrix (Fig. 7). PAN-co-PMMA/EG nanocomposites are expected to be more conductive at low filler concentrations. The conductivity of the nanocomposites was measured, and it was found that, with the addition of a small amount of EG (1 to 4 mass%), the electrical conductivity gradually increases from 2.3 to 4.8×10^{-7} S/cm. The electrical conductivity of nanocomposites gradually increases with an increase in graphite loading. The increase in conductivity from 2 to 4 mass% reveals the occurrence of a percolation threshold. This low percolation concentration also reveals a good dispersion of EG in the PAN-co-PMMA matrix. From Fig. 8, the impedance of the PAN-co-PMMA /EG nanocomposites was found to be reduced with an increase in the EG loading from 1 to 4 mass%, which was attributed to an increase in the conductivity of the nanocomposites.

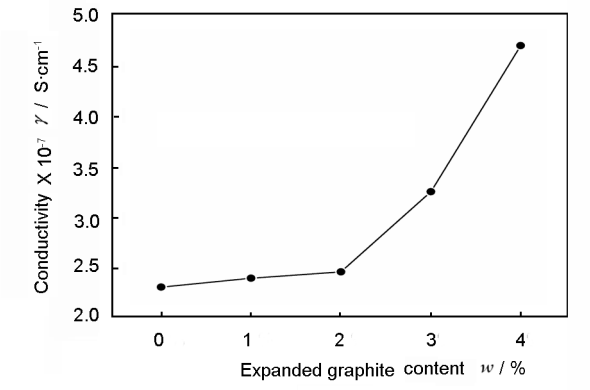

Fig. 7 Electrical conductivity of PAN-co-PMMA/EG nanocomposite with different mass fractions of EG

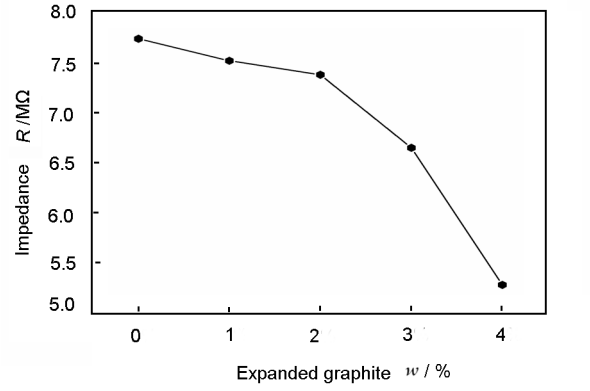

Fig. 8 Electrical impedance of the PAN-co-PMMA/EG nanocomposite with different mass fractions of EG

3.5 Oxygen permeability of PAN-co-PMMA/EG nanocomposites

The oxygen permeability of virgin PAN-co-PMMA and PAN-co-PMMA/EG nanocomposites is depicted in Fig. 9.

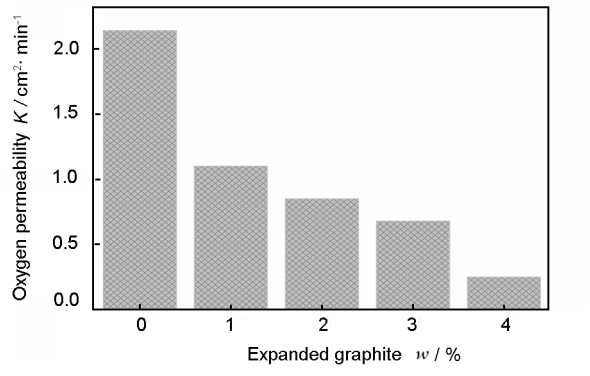

Fig. 9 Oxygen permeability of PAN-co-PMMA/EG nanocomposite with different mass fractions of EG at a constant pressure of 1.37×10^4 Pa

The oxygen flow rate through all the nanocomposites was observed to be less as compared with the virgin PAN-co-PMMA up to 1.72×10^4 Pa. In Fig. 9, the permeability of 1.37×10^4 Pa versus EG (mass%) at a constant pressure indicated that the permeability of PAN-co-PMMA/EG nanocomposites was substantially reduced when the EG content increased from 1 to 4%. The permeability of PAN-co-PMMA/EG nanocomposites was substantially reduced by 8 times with an increase in the EG content. This is caused due to the fact that the graphene nanoplatelets created a tortuous path for the permeation of oxygen gas through the nanocomposites.

4 Conclusions

PAN-co-PMMA/EG gas barrier nanocomposites were prepared by a low-cost and a green emulsifier-free emulsion polymerization method. The properties of the nanocomposites were sensitive to the inter-connectivity of EG, which was directly related to electrical conductivity. The electrical conductivity of the nanocomposites increases even with the addition of a small amount of graphite. In addition, the oxygen permeability of the nanocomposites decreases substantially with an increase in the EG content.

Acknowledgments

The authors are thankful to BRNS, DAE, and the Government of India for providing financial support under Grant OM # 2008/20/37/5/BRNS/1936. They are also thankful to the UGC for providing financial support under the SAP program.

References

[1] Alexandre M, Dubosis P. Polymer-layered silicate nanocomposites: preparation, properties and uses of a new class of materials [J]. Mater Sci Eng, 2000, 28: 1-63.

[2] Kojima Y, Usuki A, Kawasami M. Mechanical properties of nylon-6-clay hybrid[J]. J Mater Res, 1993, 8: 1185-1189.

[3] Srivastav S K, Pramanik M, Acharya H. Ethylene/Vinyl acetate copolymer/clay nanocomposites[J]. J Polym Sci Part B: Polym Phys, 2006, 44: 471-480.

[4] Gabriel P, Cipriano L G, Ana J M. Polymer composites prepared by compression molding of a mixture of carbon black and nylon 6 powder[J]. Polym Comp, 1999, 20: 804-808.

[5] Du F, Scogna R C, Zhou W, et al. Nanotube networks in polymer nanocomposites: v Rheology and electrical conductivity[J]. Macromolecules, 2004, 37: 9048-9055.

[6] Mamunya E P, Davidenko V V, Lebedev E V. Effect of polymer-filler interface interactions on percolation conductivity of thermo plastics with carbon black[J]. Comp Inter, 1996, 4: 169-176.

[7] Hirata M, Gotou T, Horiuchi S, et al. Thin-film particles of graphite oxide 1: High-yield synthesis and flexibility of the parti-

cles[J]. Carbon, 2004, 42: 2929-2937.
[8] Zhang Y, Tan Y W, Stormer H L, et al. Experimental observation of the quantum hall effect and Berry's phase in graphene [J]. Nature, 2005, 438: 201-204.
[9] Zhang Y, Small J P, Amori M E S, et al. Electric field modulation of galvanomagnetic properties of mesoscopic graphite[J]. Phys Rev Lett, 2005, 94: 176803-1-176803-4.
[10] Zheng W, Wong S C, Sue H J. Transport behaviour of PMMA/expanded graphite nanocomposites[J]. Polymer, 2002, 43: 6767-6773.
[11] Dresselhaus M S, Dresselhaus G. Intercalation compounds of graphite[J]. Adv Phys, 2002, 51: 1-186.
[12] Yu A P, Ramesh P, Itkis M E, et al. Graphite nanoplatelet-epoxy composite thermal interface materials[J]. J Phys Chem C, 2007, 111: 7565-7569.
[13] Pan Y X, Yu Z Z, Ou Y C, et al. A new process of fabricating electrically conducting nylon 6/ graphite nanocomposites via intercalation[J]. J Polym Sci Part B: Polym Phys, 2000, 38 (12): 1626-1633.
[14] Ishigure Y, Iijima S, Ito H, et al. Electrical and elastic properties of conductor-polymer composites[J]. J Mater Sci, 1999, 34: 2979-2985.
[15] Pinto G, Martin A J. Conducting aluminum-filled nylon 6 composites[J]. Polym Compos, 2001, 22: 65-70.
[16] Roldughin V I, Vysotskii V V. Percolation properties of metal-filled polymer films, structure and mechanisms of conductivity [J]. Prog Org Coat, 2000, 39: 81-100.
[17] Giannelis E P. Polymer layered silicate nanocomposites[J]. Adv Mater, 1996, 8: 29-35.
[18] Lebaron P C, Wang Z, Pinnavaia T. Polymer-layered silicate nanocomposites: An overview[J]. Appl Clay Sci, 1999, 15: 11-29.
[19] Wang C, Guo Z X, Fu S, et al. Polymers containing fullerene or carbon nanotube structures[J]. Prog Polym Sci, 2004, 29: 1079-1141.
[20] Ajayan P M, Schadler L S, Giannaris C, et al. Single-walled carbon nanotube-polymer composites: Strength and Weakness [J]. Adv Mater, 2000, 12: 750-753.
[21] Thostenson E T, Ren Z, Chou T W. Advances in the science and technology of carbon nanotubes and their composites[J]. Compos Sci Techno, 2001, 61: 1899-1912.
[22] Berber O, Sundararaj U. Big returns from small fibers: a review of polymer/carbon nanotube composites[J]. Polym Compos, 2004, 25: 630-645.
[23] Stankovich S, Piner R D, Chen X Q, et al. Stable aqueous dispersions of graphitic nanoplatelets via the reduction of exfoliated graphite oxide in the presence of Poly (sodium 4-styrenesulfonate) [J]. J Mater Chem, 2006, 16: 155-158.
[24] Chiang C L, Hsu S W. Novel epoxy/expandable graphite halogen-free flame retardant composites-preparation, characterization and properties[J]. J Polym Res, 2010, 17: 315-323.
[25] Paredes J I, Villar-Rodil S, Martinez-Alonso A, et al. Graphene oxide dispersions in organic solvents[J]. Langmuir, 2008, 24: 10560-10564.
[26] Zhao X, Zhang Q, Chen D. Enhanced mechanical properties of graphene-based poly (vinyl alcohol) composites[J]. Macromolecules, 2010, 43: 2357-2363.

纳米石墨片/共聚物复合材料及其耐热、导电和气密性

Gyanaranjan Prusty[1], Sarat K Swain[1,2]

(1. Department of Chemistry, North Orissa University, Takatpur, Baripada 757003, India;
2. Department of Chemistry, Veer Surendra Sai University of Technology, Burla, Sambalpur 768018, India)

摘　要: 通过原位乳化聚合制备了不同膨胀石墨含量(1%、2%、3%和4%质量分数)的聚丙烯腈-聚甲基丙烯酸甲酯共聚物/膨胀石墨纳米复合材料。通过紫外-可见和傅里叶变换红外光谱验证了共聚物及纳米复合材料结构的形成。用X射线衍射、扫描电镜、透射电镜研究了膨胀石墨在聚合物基体中的分散性及其形貌。用热重考察了复合材料的耐热稳定性,同时也考察了复合材料的电导特性及其阻抗随膨胀石墨含量的变化规律。研究表明,随着复合材料中石墨含量的增加,复合材料的氧气密性和热稳定性获得较大程度的改善。

关键词: 纳米复合材料;聚丙烯腈-聚甲基丙烯酸甲酯共聚物;膨胀石墨;气密性;热重分析

通讯作者: Sarat K Swain. 传真: 06792-255127, E-mail: swainsk2@yahoo.co.in

作者介绍: Gyanaranjan Prusty(1985-),男,博士研究生,从事聚合物纳米复合材料的研究. E-mail: gyanaranjan.bapu@gmail.com